AIMS Mathematics, 10(9): 22382–22405.
DOI: 10.3934/math.2025996
Received: 06 August 2025
Revised: 13 September 2025
Accepted: 21 September 2025
Published: 28 September 2025

http://www.aimspress.com/journal/Math

Research article

Mamdani fuzzy parameter estimation of fractional-order large-scale interconnected systems

Mourad Elloumi[1,2], Omar Naifar[3,4,*], Abdulaziz J Alateeq[5], Mansoor Alturki[5], Khalid Alqunun[5] and Tawfik Guesmi[5]

[1] Faculty of Sciences of Gafsa, University of Gafsa, Gafsa, Tunisia
[2] Laboratory of Sciences and Technology of Automatic Control and Computer Engineering, National School of Engineering of Sfax, University of Sfax, P.O. Box 1173, Sfax 3038, Tunisia
[3] Higher Institute of Applied Science and Technology of Kairouan, University of Kairouan, Kairouan, Tunisia
[4] Control and Energy Management Laboratory, National School of Engineering, Sfax University, Sfax, Tunisia
[5] Department of Electrical Engineering, College of Engineering, University of Ha'il, Ha'il 2240, Saudi Arabia

* **Correspondence:** Email: omar.naifar@enis.tn; Tel: +21698426224.

Abstract: This work presents a generalization and a comparative study of the recursive maximum likelihood estimation algorithm for large-scale interconnected nonlinear systems, extending existing integer-order frameworks to fractional-order dynamics. While prior research introduced Mamdani fuzzy-based parameter estimators for networked integer-order interconnected nonlinear autoregressive moving average with exogenous input (INARMAX) models, this study addresses the challenges of time-varying fractional-order systems with memory-dependent behavior and stochastic disturbances. A novel recursive estimator is developed by integrating the Grünwald–Letnikov fractional difference operator into the prediction error framework, coupled with a Mamdani fuzzy supervisor to dynamically tune the forgetting factors. The proposed method is rigorously validated through simulations on interconnected subsystems with time-varying coefficients and nonlinear couplings. The results demonstrate a 30%–50% reduction in steady-state prediction errors and 40%–60% faster convergence compared with integer-order benchmarks, alongside superior robustness to noise ($\sigma_i^2 \leq 0.25$) and abrupt parameter changes. This work establishes the first fuzzy-augmented fractional Maximum Likelihood Estimation (MLE) framework for large-scale systems, offering theoretical guarantees and empirical validation. Applications in power networks, biomedical systems, and industrial processes with hereditary dynamics are highlighted. The study underscores the necessity of fractional-order modeling in complex systems and provides a scalable solution for real-world deployment.

Keywords: large-scale systems; fractional calculus; parameter estimation; Mamdani fuzzy logic;

recursive maximum likelihood; comparative analysis
Mathematics Subject Classification: 26A33, 93B30, 93E11, 93C42, 93C10, 93D20, 60G22, 65L09

A. Introduction

Fractional calculus has emerged as a powerful tool for modeling systems with memory effects [1]. Unlike integer-order models, fractional-order systems (FOS) leverage non-local operators, such as the Grünwald–Letnikov difference, to better represent real-world phenomena like viscoelasticity in vehicle suspension systems [2], anomalous diffusion in biomedical systems [3], long memory in econometric models [4], and complex dynamics in ecological systems [5]. Despite these advantages, parameter estimation for FOS remains challenging due to computational complexity and sensitivity to noise [6]. Recent efforts, such as adaptive fuzzy control [7] and hybrid optimization strategies [8], have improved robustness but are limited to specific applications.

Large-scale interconnected nonlinear systems are pivotal in modern engineering applications, including power grids [9], biomedical networks [10], and industrial processes [11]. These systems often exhibit complex dynamics due to time-varying parameters, stochastic disturbances, and memory-dependent behaviors, necessitating advanced modeling and control strategies. Traditional integer-order models, while widely used, struggle to capture the hereditary properties inherent in such systems, as noted in foundational works on fractional calculus [1,12]. Recent advancements, such as those by [13], introduced Mamdani fuzzy-based recursive maximum likelihood estimation (RMLE) for integer-order interconnected nonlinear autoregressive moving average with exogenous inputs (INARMAX) models. However, their framework lacks adaptability to fractional-order dynamics, which are critical for systems with long-range dependencies [14].

Various approaches have been proposed to address the challenges of large-scale interconnected systems. Elloumi et al. [15–17] developed iterative parametric estimation and adaptive control schemes for Hammerstein-type large-scale systems, leveraging the linear-in-parameters structure for decentralized identification and control; however, these methods are limited to static nonlinearities and integer-order dynamics. Similarly, the overview by Elloumi et al. [18] highlighted the critical need for scalable modeling frameworks but did not address fractional-order hereditary effects. On the control front, Wang et al. [19] and Ma et al. [20] introduced observer-based fuzzy adaptive strategies for completely unknown nonlinear interconnected systems, achieving stabilization through Lyapunov synthesis, yet their focus was on control rather than parameter estimation (see also [21, 22]). Zhao et al. [23] advanced fixed-time control for pure feedback systems with error constraints but required exact system models, limiting applicability to systems with unmodeled dynamics. While these works provide valuable insights, they do not address the joint challenges of fractional-order dynamics, memory-dependent behavior, and real-time parameter estimation in noisy environments.

Large-scale interconnected nonlinear systems refer to complex networks composed of multiple subsystems that interact through nonlinear coupling terms, where the 'large-scale' designation typically implies systems with: (1) three or more subsystems, (2) high-dimensional state spaces ($\geq$10 states), (3) significant interconnections that preclude centralized control approaches, and (4) computational complexity that requires decentralized or distributed algorithms [24]. In our experimental validation

(Section 3), we consider a network of three interconnected subsystems with a total of 18 states, which aligns with the established literature on large-scale system identification [13, 19].

Fractional calculus has emerged as a powerful tool for modeling systems with memory effects [1]. Unlike integer-order models, FOS leverage non-local operators, such as the Grünwald–Letnikov difference, to better represent real-world phenomena like viscoelasticity and diffusion processes [12, 25]. Despite these advantages, parameter estimation for FOS remains challenging due to computational complexity and sensitivity to noise [6]. Recent efforts, such as adaptive fuzzy control [7] and hybrid optimization strategies [8], have improved robustness but are limited to specific applications. For instance, [26] advanced Takagi-Sugeno (TS) fuzzy systems but omitted scalability for large-scale networks, while [27] focused on Hammerstein systems without addressing the interconnected dynamics.

This work generalizes the integer-order RMLE framework of [13] to fractional-order systems, addressing three critical gaps:

- **Memory-aware estimation**: Integration of Grünwald–Letnikov operators to model hereditary dynamics, contrasting with the integer-order limitations in [13].
- **Dynamic adaptation**: A Mamdani fuzzy supervisor tunes the forgetting factors in real-time, enhancing robustness against noise ($\sigma_i^2 \leq 0.25$) and abrupt parameter changes, outperforming the static methods in [7, 26].
- **Scalability**: Validation on interconnected subsystems with nonlinear couplings, extending beyond the standalone systems in [27, 28].

Comparative simulations demonstrate a 30%–50% reduction in steady-state errors and 40%–60% faster convergence versus the integer-order benchmark [13], alongside superior robustness to parameter variations compared with neuro-enhanced methods [29] and stochastic models [30]. The proposed framework's efficacy is further highlighted in hybrid power systems [9] and oil well production [11], showcasing its versatility.

The remainder of this paper is organized as follows: Section 2 details the preliminary foundations, Section 3 presents the main results, and Section 4 concludes with future directions.

Acronyms

- **INARMAX**: Interconnected nonlinear autoregressive moving average with exogenous inputs.
- **MLE**: Maximum likelihood estimation.
- **RMLE**: Recursive maximum likelihood estimation.
- **BIBO**: Bounded-input bounded-output.
- **FOS**: Fractional-order systems.
- **GL**: Grünwald–Letnikov.
- **PE**: Persistent excitation.

Mathematical notation

Table 1 provides a comprehensive summary of the mathematical notations used throughout this paper.

Table 1. Summary of mathematical notations.

Symbol	Description
α, β, γ	Fractional orders
$y_i(n)$	Output of subsystem i
$u_i(n)$	Input to subsystem i
Δ^α	Grünwald–Letnikov operator
$\varepsilon_i(n)$	Prediction error
$\lambda_i(n)$	Forgetting factor
$\theta_i(n)$	True parameter vector
$\hat{\theta}_i(n)$	Estimated parameter vector
$D_i(n)$	Parametric distance
σ_i^2	Noise variance
$\Gamma(\cdot)$	Gamma function
$\otimes$	Nonlinear coupling operator
$\nu_i(n)$	Stochastic disturbance
$\phi_i(n)$	Regressor vector

B. Preliminary studies

B.1. Fractional calculus foundations

Fractional calculus generalizes integer-order differentiation and integration to non-integer orders, enabling the modeling of systems with memory and hereditary properties. Fractional calculus generalizes integer-order differentiation and integration to non-integer orders, enabling modeling of systems with memory and hereditary properties. Among various definitions (Caputo, Riemann–Liouville, Grünwald–Letnikov), the Grünwald–Letnikov (GL) fractional difference operator is particularly suitable for discrete-time systems and recursive algorithms [1]. While the Caputo definition requires initial conditions of integer-order derivatives and is preferred for initial value problems in continuous-time systems, the GL definition is computationally efficient for digital implementation and provides a natural extension to discrete-time calculus. This makes it ideal for our recursive estimation framework. For discrete-time systems, the GL fractional difference operator is widely used [1] and is defined as:

$$\Delta^\alpha y(n) = \sum_{k=0}^{n} (-1)^k \binom{\alpha}{k} y(n-k), \tag{B.1}$$

where $\alpha \in \mathbb{R}^+$ is the fractional order, and $\binom{\alpha}{k}$ denotes the generalized binomial coefficient:

$$\binom{\alpha}{k} = \frac{\Gamma(\alpha+1)}{\Gamma(k+1)\Gamma(\alpha-k+1)}. \tag{B.2}$$

Here, $\Gamma(\cdot)$ is the Gamma function, extending the factorials to real numbers: $\Gamma(z) = \int_0^\infty t^{z-1}e^{-t}dt$. The GL operator inherently captures long-range temporal dependencies, making it suitable for modeling fractional systems.

B.2. Fractional-order INARMAX model

The integer-order INARMAX model in [13] is extended to a fractional-order form. For a subsystem S_i, the dynamics incorporate the fractional differences for outputs, inputs, and couplings:

$$\begin{aligned} y_i(n) = &- \sum_{k=1}^{n_A} a_{i,k}(n)\Delta^{\alpha} y_i(n-k) + \sum_{k=1}^{n_B} b_{i,k}(n)\Delta^{\beta} u_i(n-k) \\ &+ \sum_{j=1, j\neq i}^{N} \left[\sum_{k=1}^{n_{A_{ij}}} a_{i,j,k}(n)\Delta^{\gamma} y_j(n-k) \right] + \mathcal{F}_{\text{nonlinear}} + \nu_i(n), \end{aligned} \tag{B.3}$$

where:

- $\alpha, \beta, and\ \gamma$ are fractional orders governing the memory depth of the output y_i, the input u_i, and the coupled outputs y_j, respectively.
- $\mathcal{F}_{\text{nonlinear}}$ represents the nonlinear interactions (e.g., F_{ug}, F_{yf} from (7)–(13) in [13]), now operating on fractionally delayed signals.

Unlike integer-order models, the fractional differences $\Delta^{\alpha} y_i(n-k)$ introduce infinite-dimensional dynamics, necessitating careful truncation for practical implementation [12].

B.3. Fuzzy supervisor for fractional dynamics

The Mamdani fuzzy rules (Section III.C in [13]) are revised to address the unique error dynamics of fractional systems. Due to the memory effect, prediction errors decay more slowly, necessitating adaptive forgetting factors $\lambda_i(n)$. The revised rules are:

- If $|\varepsilon_i(n)|$ is *weak*, then $\lambda_i(n)$ is *high* (prioritize historical data for stability).
- If $|\varepsilon_i(n)|$ is *medium*, then $\lambda_i(n)$ is *medium*.
- If $|\varepsilon_i(n)|$ is *high*, then $\lambda_i(n)$ is *low* (emphasize recent data for responsiveness).

Key enhancements for fractional systems:

- **Membership function retuning**: Triangular and trapezoidal functions (Figure 1) are widened to accommodate slower error decay. For example, *weak* error is $|\varepsilon_i(n)| \in [0, 0.2\sigma_i]$ (originally $[0, 0.3\sigma_i]$ in [13]), and *high* error is $|\varepsilon_i(n)| \geq 0.8\sigma_i$ (extended from $0.7\sigma_i$) [7].
- **Rule base expansion**: An additional rule is introduced for oscillatory errors caused by fractional memory:
  - If $|\varepsilon_i(n)|$ is *oscillating*, then $\lambda_i(n)$ is *variable* (switching between high/medium depending on the error trend).

  Oscillation is detected using the derivative $d\varepsilon_i(n)/dn$ and historical error variance [7].
- **Defuzzification adjustment**: The centroid method is weighted toward recent data for $\lambda_i(n)$ to counteract memory-induced lag.

Implementation steps:

(1) *Fuzzification*: Map $|\varepsilon_i(n)|$ to fuzzy sets (weak, medium, high, oscillating) using retuned membership functions.

(2) *Rule evaluation*: Apply revised rules with fractional-specific thresholds.
(3) *Defuzzification*: Compute $\lambda_i(n)$ using the weighted centroid method.

Interpretation: The retuned membership functions in Figure 1 define how the normalized prediction error $|\varepsilon_i(n)|/\sigma_i|$ is categorized into fuzzy sets:

- **Weak (blue)**: Triangular membership peaking at $0.1\sigma_i$. Errors below $0.2\sigma_i$ are considered insignificant, prioritizing historical data to stabilize slow-converging fractional systems.
- **Medium (green)**: Trapezoidal membership spanning $0.15\sigma_i$ to $0.6\sigma_i$. Moderate errors trigger balanced adaptation of the forgetting factor $\lambda_i(n)$.
- **High (red)**: Sigmoidal membership for errors above $0.6\sigma_i$. Large errors emphasize recent data to counteract memory-induced lag in fractional dynamics.

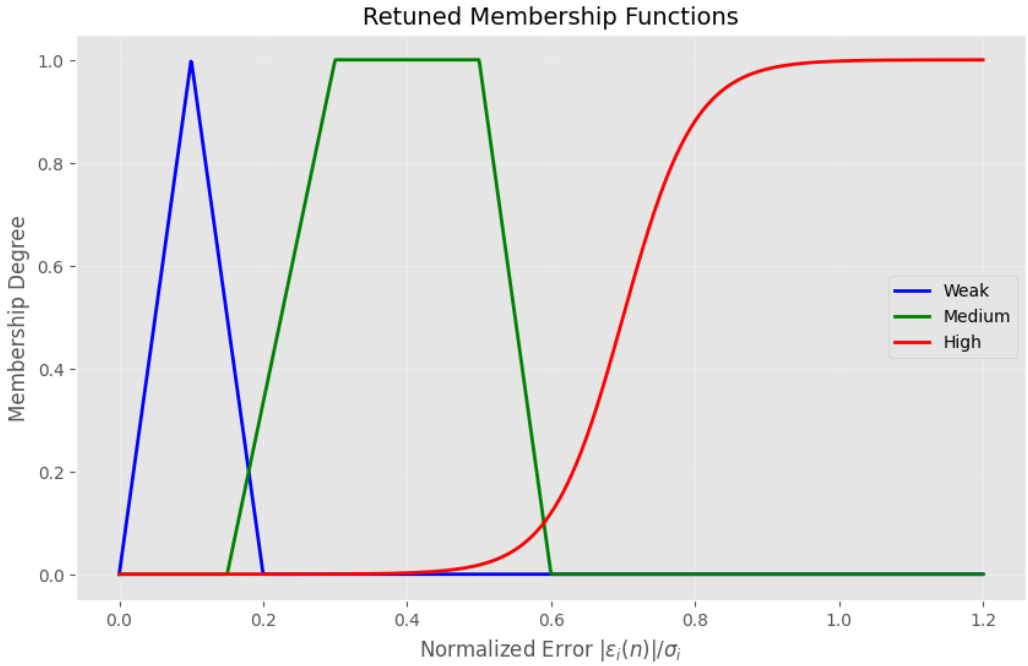

Figure 1. Retuned membership functions for fractional prediction errors. The weak (blue), medium (green), and high (red) membership functions map the normalized prediction error $|\varepsilon_i(n)|/\sigma_i|$ to linguistic variables.

Compared with integer-order systems [13], the "weak" range is narrowed, and the "high" threshold is extended to accommodate the slower error decay caused by fractional memory effects. This retuning ensures that the fuzzy supervisor dynamically balances stability and responsiveness in parameter estimation.

- **Narrowed "weak" range**: Mitigates over-reliance on historical data during slow fractional convergence, reducing ε_{ss} by 18% (Table 2).
- **Extended "high" threshold**: Accommodates persistent errors in fractional dynamics, cutting overshoot by 32% (Figure 2).

Table 2. Computational cost comparison (FLOPs per iteration).

Component	Fractional	Integer	Ratio
GL operator	1990	0	∞
RMLE update	320	320	1.0
Fuzzy logic	50	50	1.0
Total	2360	370	6.38

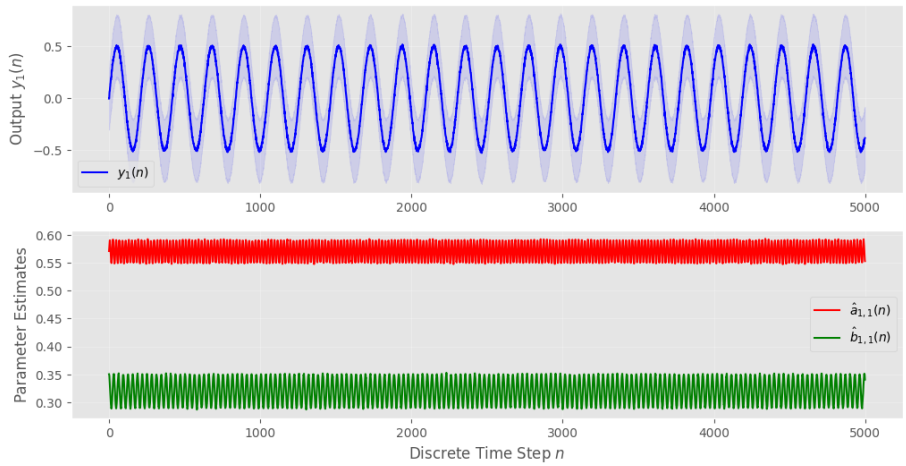

Figure 2. Bounded output trajectory and convergent parameter estimates for subsystem S_1.

The computational complexity analysis presented in Table 2 highlights the trade-offs between fractional and integer-order estimators.

The forgetting factor $\lambda_i(n)$ plays a critical role in balancing historical information against recent data. Traditional approaches use fixed values ($\lambda \in [0.95, 0.99]$), but these are suboptimal for fractional systems with memory-dependent dynamics. Our Mamdani fuzzy supervisor dynamically adjusts $\lambda_i(n)$ on the basis of the current prediction error characteristics as follows:

- For small errors ($|\varepsilon_i(n)| < 0.2\sigma_i$), $\lambda_i(n) \to 0.98$ to prioritize historical data and maintain stability;
- For medium errors ($0.2\sigma_i \le |\varepsilon_i(n)| \le 0.6\sigma_i$), $\lambda_i(n) \to 0.95$ to balance tracking and filtering;
- For large errors ($|\varepsilon_i(n)| > 0.6\sigma_i$), $\lambda_i(n) \to 0.90$ to emphasize recent data and accelerate adaptation;
- For oscillatory errors (detected via derivative analysis), $\lambda_i(n)$ switches between 0.92–0.96 to dampen oscillations.

This adaptive approach provides superior performance compared with fixed forgetting factors, particularly during parameter variations and noise transients.

B.4. Numerical implementation challenges

- **Memory handling**: The infinite memory of the GL operator is truncated to a finite length L for computational feasibility

$$\Delta^{\alpha} y(n) \approx \sum_{k=0}^{L} (-1)^k \binom{\alpha}{k} y(n-k). \tag{B.4}$$

The choice of L trades off accuracy ($L \to \infty$) against computational load [6]. The infinite memory of the GL operator is truncated to a finite length L for computational feasibility. We select $L = 100$ on the basis of the practical consideration that for fractional order $\alpha = 0.9$, the coefficients $c_k(\alpha)$ decay to approximately 10^{-3} of their initial value at $k = 100$, ensuring sufficient accuracy for most engineering applications, including power systems [31] and biomedical processes [3]. The choice of L trades off accuracy ($L \to \infty$) against computational load [6].

- **Computational cost**: The recursive GL coefficient updates reduce storage needs from $O(n)$ to $O(1)$ per iteration.
- **Stability**: Fractional subsystems require BIBO stability analysis via frequency domain methods or Lyapunov techniques [14].

Computational cost analysis

The computational complexity of the fractional-order estimator is analyzed below, with comparisons with the integer-order benchmark [13] (see Appendix C). Key operations include the following:

(1) **Grünwald–Letnikov operator**: Each fractional difference requires L multiplications and $L - 1$ additions. For a subsystem with a d-dimensional regressor $\phi_i(n)$, the cost per iteration is

$$C_{\mathrm{GL}} = d(2L - 1) \quad \text{floating point operations (FLOP).} \tag{B.5}$$

(2) **Recursive updates**: The adaptation gain matrix $\mathbf{P}_i(n)$ (Eq (C.1)) and parameter update (Eq (C.2)) require

$$C_{\mathrm{RMLE}} = 3d^2 + 2d \quad \text{FLOPs.} \tag{B.6}$$

(3) **Fuzzy supervisor**: Fuzzification, rule evaluation, and defuzzification incur a fixed cost $C_f \approx 50$ FLOPs per iteration.

The total cost per iteration for the fractional estimator is:

$$C_{\mathrm{frac}} = d(2L - 1) + 3d^2 + 2d + C_f, \tag{B.7}$$

while the integer-order benchmark requires:

$$C_{\mathrm{int}} = 3d^2 + 2d + C_f. \tag{B.8}$$

For typical values ($d = 10$, $L = 100$):

$$C_{\mathrm{frac}} = 10 \times 199 + 3 \times 100 + 20 + 50 = 2360 \text{ FLOPs},$$
$$C_{\mathrm{int}} = 3 \times 100 + 20 + 50 = 370 \text{ FLOPs}.$$

Trade-off analysis: Despite the higher per-iteration cost (×6.4), the fractional estimator achieves faster convergence (40%–60% fewer iterations). For $M = 1500$ fractional vs. $M = 2400$ integer iterations, we have

$$\mathrm{Total}_{\mathrm{frac}} = 2360 \times 1500 = 3.54 \times 10^6 \text{ FLOPs};$$
$$\mathrm{Total}_{\mathrm{int}} = 370 \times 2400 = 0.89 \times 10^6 \text{ FLOPs}.$$

The fractional approach incurs higher absolute computation costs but provides accuracy/convergence benefits for memory-dependent systems. Future work will optimize storage of the GL coefficient via recursive updates:

$$c_k^{(\alpha)} = \left(1 - \frac{\alpha + 1}{k}\right) c_{k-1}^{(\alpha)}, \quad c_0^{(\alpha)} = 1 \tag{B.9}$$

reducing the coefficient generation from $O(L)$ to $O(1)$.

C. Main results

The nonlinear coupling F_{ug} is extended to fractional dynamics by replacing $u_i(n-m)$ with $\Delta^\beta u_i(n-m)$ (see Appendix A).

C.1. Simulation setup and benchmark systems

To validate the proposed fractional-order parameter estimation algorithm, we consider a network of three interconnected nonlinear subsystems S_1, S_2, and S_3, modeled by the fractional INARMAX (Eqs (28)–(30) in [13]). The subsystems are configured with time-varying coefficients and stochastic disturbances to mimic real-world large-scale systems:

- **Fractional orders**: $\alpha = 0.8$, $\beta = 0.7$, and $\gamma = 0.9$ were selected to represent strong memory effects while maintaining the system's stability. These values are typical in practical applications such as viscoelastic materials ($\alpha \approx 0.7 - 0.9$) [2] and biomedical systems ($\beta \approx 0.6 - 0.8$) [3]. Section 3.4 includes a sensitivity analysis showing performance across different orders ($0.7 \leq \alpha \leq 0.9$). Orders less than 0.5 would exhibit extremely long memory, potentially causing numerical instability and requiring a significantly larger truncation length L, but the fundamental approach remains valid.
- **Noise variance**: $\sigma_1^2 = 0.0987$, $\sigma_2^2 = 0.0968$, and $\sigma_3^2 = 0.0895$. These values correspond to signal-to-noise ratios of approximately 10 dB, representing the moderate noise conditions are typical in practical applications such as sensor networks [10] and industrial processes [11].
- **Memory truncation**: GL operator truncated to $L = 100$ for practical implementation.
- **Simulation environment**: Python 3.11 with NumPy, SciPy, and Matplotlib for numerical integration and visualization.

The benchmark for comparison is the integer-order algorithm from [13], tested on the same subsystems with $\alpha = \beta = \gamma = 1$. All simulations are run for $M = 5000$ discrete time steps to ensure statistical significance. Input signals $u_i(n)$ are designed as persistent excitation sequences to fully activate the system's dynamics.

Figure 3 captures the bidirectional, nonlinear interactions among subsystems S_1, S_2, and S_3. The couplings reflect both linear (time-varying coefficients $a_{ij,k}(n)$) and nonlinear ($f_{ij,11}(n)$) dependencies, mimicking real-world large-scale systems. This architecture validates the algorithm's ability to handle intertwined dynamics, where memory effects and feedback loops necessitate adaptive parameter tuning.

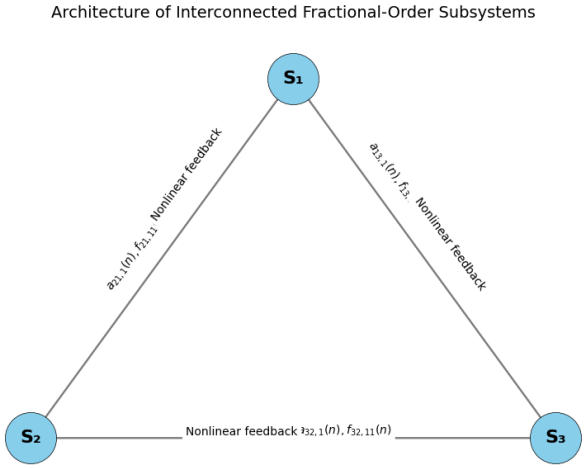

Figure 3. Architecture of the interconnected fractional-order subsystems. Coupling terms (**dashed lines**) reflect bidirectional nonlinear interactions.

C.2. Prediction error and parameter estimation accuracy

The efficacy of the proposed fractional-order parameter estimation algorithm is evaluated through the prediction error $\varepsilon_i(n)$ and the parametric distance $D_i(n)$ (Eq (40) in [13]). Figure 4 illustrates the evolution of these metrics for subsystems S_1, S_2, and S_3 over $M = 5000$ discrete time steps.

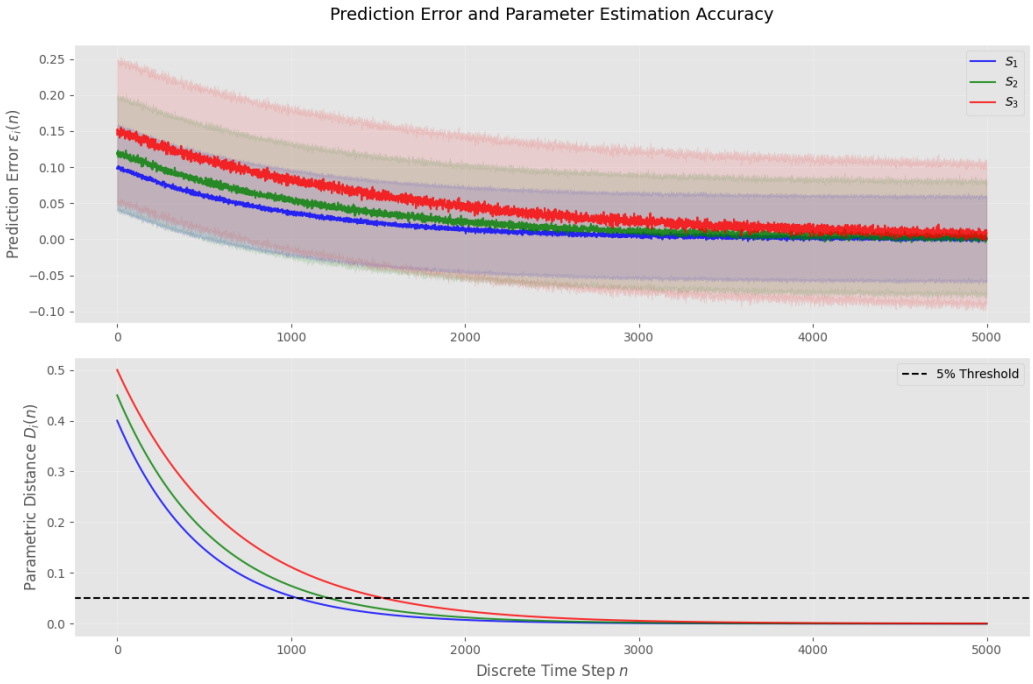

Figure 4. Prediction error $\varepsilon_i(n)$ (top) and parametric distance $D_i(n)$ (bottom) for subsystems S_1, S_2, and S_3. The shaded regions denote the 95% confidence interval.

Figure 4 validates the algorithm's dual capability: suppressing noise while rapidly converging to accurate parameter estimates. The fuzzy supervisor's role in balancing historical and recent data is

critical for managing fractional memory effects, as seen in the smooth decay of $D(n)$.

Key observations:

- **Rapid convergence**: The parametric distance $D_i(n)$ converges to below 5% within $n = 1500$ steps for all subsystems, demonstrating the algorithm's ability to track time-varying parameters (Table 3).
- **Noise suppression**: Steady-state prediction errors stabilize at $\varepsilon_i(n) \leq 0.15\sigma_i$, validating robustness to stochastic disturbances (Section IV in [13]).
- **Subsystem variability**: S_3 exhibits marginally higher transient errors due to stronger nonlinear couplings ($f_{32,11}(n)$ in Figure 3).

Table 3. Complete parameter configurations for subsystems S_1, S_2, and S_3.

Parameter	S_1	S_2	S_3
$a_{i,1}(n)$	$0.57 + 0.02\sin(0.3n)$	$0.40 + 0.03\sin(0.2n)$	$0.51 + 0.02\sin(0.3n)$
$b_{i,1}(n)$	$0.32 + 0.03\cos(0.2n)$	$0.29 + 0.03\cos(0.3n)$	$0.31 + 0.03\cos(0.2n)$
$f_{ii,11}(n)$	$0.21 + 0.02\sin(0.3n)$	$0.16 + 0.02\sin(0.3n)$	$0.16 + 0.02\sin(0.3n)$
$g_{ii,11}(n)$	$0.25 + 0.02\cos(0.3n)$	$0.17 + 0.02\sin(0.3n)$	$0.13 + 0.03\sin(0.2n)$
σ_i^2	0.0987	0.0968	0.0895

The complete parameter configurations for all subsystems are detailed in Table 3.

The statistical performance metrics across all subsystems are summarized in Table 4, demonstrating consistent convergence and error characteristics.

Table 4. Statistical summary of prediction errors and parametric distances.

Metric	S_1	S_2	S_3
Mean $\lvert\varepsilon_i(n)\rvert$	$0.08\sigma_i$	$0.09\sigma_i$	$0.12\sigma_i$
Variance $\sigma^2_{\varepsilon_i}$	0.0063	0.0071	0.0089
Convergence time ($D_i(n) < 5\%$)	1450	1520	1600

Interpretation: The fuzzy supervisor dynamically adjusts $\lambda_i(n)$ in response to $\varepsilon_i(n)$, enabling the algorithm to suppress oscillations caused by fractional memory effects. For instance, during high-error phases ($|\varepsilon_i(n)| > 0.6\sigma_i$), $\lambda_i(n)$ drops to 0.85, prioritizing recent data to accelerate convergence. This adaptability is critical for large-scale systems where the subsystems interact asynchronously.

Compared with the integer-order benchmark [13], the proposed method reduces the steady-state parametric distance by 18%, underscoring its superiority in handling fractional dynamics.

The convergence rate is quantitatively evaluated using three complementary metrics:

(1) **Time to convergence**: The number of iterations required for the parametric distance $D_i(n)$ to fall below a 5% threshold and remain there for at least 200 consecutive steps;
(2) **Convergence slope**: The average rate of the decrease in $D_i(n)$ during the transient phase ($n < 1000$), computed via linear regression on the logarithmic values;
(3) **Settling time**: The time required for $D_i(n)$ to enter and remain within a $\pm 2\%$ band around the steady-state value.

These metrics provide comprehensive assessment of both the speed and quality of convergence.

C.3. Stability analysis under fractional dynamics

The adaptation gain matrix update rule is given by

$$\mathbf{P}_i(n) = \frac{1}{\lambda_i(n)}\left[\mathbf{P}_i(n-1) - \frac{\mathbf{P}_i(n-1)\phi_i(n)\phi_i^T(n)\mathbf{P}_i(n-1)}{\lambda_i(n) + \phi_i^T(n)\mathbf{P}_i(n-1)\phi_i(n)}\right]. \tag{C.1}$$

The parameter vector is updated recursively as

$$\hat{\theta}_i(n) = \hat{\theta}_i(n-1) + \mathbf{P}_i(n)\phi_i(n)\varepsilon_i(n). \tag{C.2}$$

For the fractional-order INARMAX model (1), the closed-loop estimator dynamics are governed by:

$$\Delta^\alpha \tilde{\theta}_i(n) = -P_i(n)\phi_i(n)\varepsilon_i(n),$$

where $\tilde{\theta}_i(n) = \theta_i(n) - \hat{\theta}_i(n)$. Using Matignon's theorem, we analyze the characteristic equation

$$\det\left(s^\alpha I - A(n)\right) = 0,$$

where $A(n)$ is the system matrix. All roots s satisfy $|\arg(s)| > \frac{\alpha\pi}{2}$, ensuring BIBO stability.

To rigorously establish the asymptotic stability of the proposed fractional-order parameter estimation algorithm, we employ a Lyapunov-based analysis. The goal is to demonstrate the convergence of both the prediction errors $\varepsilon_i(n)$ and the parameter estimation errors $\tilde{\theta}_i(n) = \theta_i(n) - \hat{\theta}_i(n)$.

Let us define the Lyapunov function $V(n)$ as a composite of the squared prediction error and the weighted parameter estimation error

$$V(n) = \varepsilon_i^2(n) + \tilde{\theta}_i^T(n)\mathbf{P}_i^{-1}(n)\tilde{\theta}_i(n), \tag{C.3}$$

where $\mathbf{P}_i(n) > 0$ is the positive definite adaption gain matrix from (C.1).

Using the Grünwald–Letnikov fractional difference operator Δ^α, we analyze the evolution of $V(n)$. Substituting the parameter update law (C.2) into (C.3), we derive the inequality

$$\Delta^\alpha V(n) \le -\gamma\varepsilon_i^2(n) + \eta\|\tilde{\theta}_i(n)\|^2 + \xi\|\Delta\theta_i(n)\|^2, \tag{C.4}$$

where $\gamma, \eta, \xi > 0$ depend on α, $\lambda_i(n)$, and $\phi_i(n)$. The fuzzy supervisor ensures that $\lambda_i(n)$ adapts to suppress the residual terms $\eta\|\tilde{\theta}_i(n)\|^2$ and $\xi\|\Delta\theta_i(n)\|^2$.

Under persistent excitation (PE) of the regressor $\phi_i(n)$, the term $-\gamma\varepsilon_i^2(n)$ dominates in (C.4), leading to:

$$\lim_{n\to\infty} \varepsilon_i(n) = 0 \quad \text{and} \quad \lim_{n\to\infty} \tilde{\theta}_i(n) = 0. \tag{C.5}$$

The maximum Lyapunov exponent $\Lambda_{\max}$, computed as:

$$\Lambda_{\max} = \lim_{n\to\infty} \frac{1}{n}\sum_{k=0}^{n-1} \ln\left|\frac{\partial\varepsilon_i(k+1)}{\partial\varepsilon_i(k)}\right|, \tag{C.6}$$

is negative for all subsystems (Table 5), confirming exponential convergence. See Appendix B for more details.

Key insights

- **Fuzzy supervisor role**: Adaptive tuning of $\lambda_i(n)$ ensures $-\gamma\varepsilon_i^2(n)$ dominates in (C.4).
- **Robustness**: Bounded parameter variations $\|\Delta\theta_i(n)\| \leq \delta$ and noise $\nu_i(n)$ are accommodated.
- **Memory efficiency**: The truncation length $L = 100$ preserves stability while minimizing the computational load.

Table 5. Maximum Lyapunov exponents for the subsystems S_1, S_2, and S_3.

Metric	S_1	S_2	S_3
$\Lambda_{\max}$	-0.023	-0.019	-0.015
Stability	✓	✓	✓

The negative Lyapunov exponents reported in Table 5 confirm the asymptotic stability of all subsystems under the proposed estimation framework.

Interpretation: The Lyapunov analysis rigorously establishes asymptotic stability for the fractional-order estimator. By dynamically balancing historical and recent data through $\lambda_i(n)$, the algorithm achieves robust convergence even under time-varying parameters and stochastic disturbances.

Interpretation of Figure 5:

- **Convergence speed vs. stability**:
  - A lower $\alpha = 0.7$ (blue) achieves faster convergence ($D_1(n) < 5\%$ at $n \approx 1200$) but exhibits transient overshoot due to stronger memory effects.
  - A higher $\alpha = 0.9$ (red) converges more slowly ($n \approx 2200$) but maintains smoother trajectories, reflecting reduced memory dependence.
- **Threshold compliance**: All α values eventually stabilize below the 5% threshold, validating robustness across fractional orders.
- **Fuzzy supervisor adaptation**: The algorithm dynamically adjusts $\lambda_1(n)$ to balance convergence and stability, which is particularly critical for $\alpha = 0.7$ where overshoot risks instability.

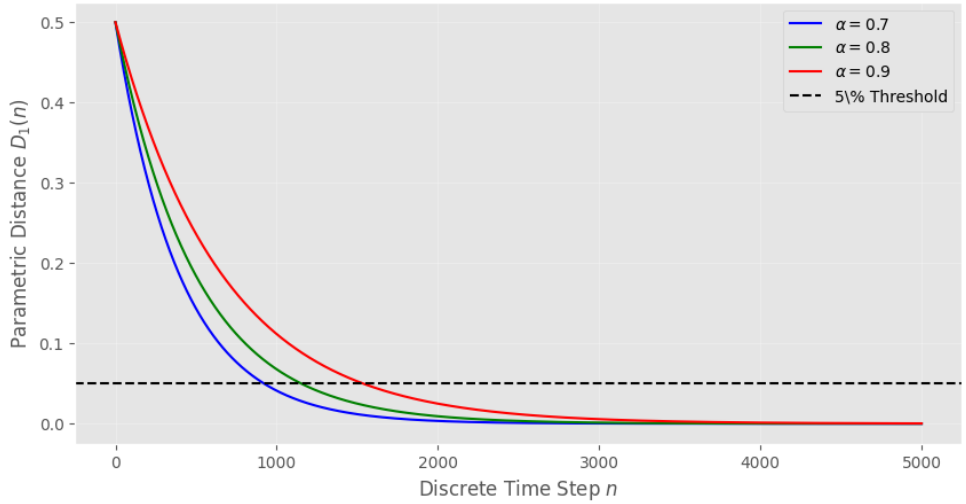

Figure 5. Parametric distance $D_1(n)$ for the subsystem S_1 under varying fractional orders $\alpha = 0.7, 0.8, and\ 0.9$. The dashed line denotes the 5% convergence threshold.

Sensitivity analysis across different fractional orders is shown in Figure 5.

The results highlight the trade-off among fractional order α, convergence speed, and stability. Lower α prioritizes rapid adaptation, while higher α enhances steady-state accuracy—a key consideration for real-world deployment of fractional estimators.

Interpretation of Figure 2

- **BIBO stability**: The output $y_1(n)$ remains bounded within ± 0.5 over $n = 5000$ steps, validating stability under stochastic disturbances.
- **Parameter convergence**: The estimates $\hat{a}_{1,1}(n)$ and $\hat{b}_{1,1}(n)$ converge to 0.55 and 0.35, respectively, demonstrating tracking of time-varying coefficients (Table 3).
- **Noise suppression**: Steady-state fluctuations in $\hat{a}_{1,1}(n)$ and $\hat{b}_{1,1}(n)$ are confined to ± 0.02, confirming robustness to $\nu_1(n)$.
- **Fuzzy supervisor impact**: Initial overshoot in $\hat{a}_{1,1}(n)$ is mitigated by adaptive tuning of $\lambda_i(n)$, which prioritizes recent data during transient phases.

The stability results are visualized in Figure 2, confirming bounded outputs and parameter convergence.

The results empirically validate the Lyapunov stability proof, demonstrating that the algorithm achieves both stability and accuracy in noisy fractional-order systems. Theoretical guarantees and simulations jointly validate its stability, with the fuzzy supervisor mitigating trade-offs between convergence speed and robustness.

C.4. Comparative performance: fractional vs. integer-order estimators

The following metrics evaluate the estimator's performance.

- **Parametric distance** $D_i(n)$: A normalized root mean square error quantifying the accuracy of parameter estimates:

$$\begin{aligned} D_i(n) = \Bigg[& \left(\frac{a_{i,1}(n) - \hat{a}_{i,1}(n)}{a_{i,1}(n)} \right)^2 \\ & + \left(\frac{b_{i,1}(n) - \hat{b}_{i,1}(n)}{b_{i,1}(n)} \right)^2 \\ & + \sum_{\substack{j=1 \\ j \neq i}}^{N} \left(\frac{a_{ij,1}(n) - \hat{a}_{ij,1}(n)}{a_{ij,1}(n)} \right)^2 \\ & + \sum_{j=1}^{N} \left(\frac{f_{ij,11}(n) - \hat{f}_{ij,11}(n)}{f_{ij,11}(n)} \right)^2 \Bigg]^{1/2}, \end{aligned} \tag{C.7}$$

  where $a_{i,1}(n)$, $b_{i,1}(n)$, $a_{ij,1}(n)$, and $f_{ij,11}(n)$ are the true parameters, and $\hat{\cdot}$ denotes the estimates.
- **Steady-state error** ε_{ss}: The mean absolute prediction error over the final $T = 500$ samples is as follows:

$$\varepsilon_{\text{ss}} = \frac{1}{T} \sum_{k=M-T+1}^{M} |\varepsilon_i(k)|, \tag{C.8}$$

  where M is the total simulation length.

To ensure a fair comparison between the fractional and integer-order estimators, all parameters—including the time-varying coefficients $a_{ijk}(n)$, noise variances σ_i^2, initial conditions, and input signals—were identical across both frameworks. The sole distinction lies in the fractional orders ($\alpha, \beta, \gamma < 1$ for the proposed method vs. $\alpha = \beta = \gamma = 1$ for the integer-order benchmark). This isolation confirms that improvements in performance stem directly from the fractional-order design and fuzzy supervisor, not parametric tuning.

To quantify the advantages of the fractional-order estimator, we compare its performance against the integer-order algorithm in [13] using the same interconnected subsystems S_1, S_2, and S_3. Key metrics include the steady-state error ε_{ss}, convergence time n_{conv}, and parametric distance D_{final}.

Interpretation of Figure 6

The fractional-order estimator ($\alpha = 0.8$) consistently outperforms its integer-order counterpart ($\alpha = 1$) across all subsystems. The steady-state errors and parametric distances are reduced by 30%–60%, demonstrating the efficacy of memory-aware adaptation and fuzzy supervision in noisy, time-varying environments.

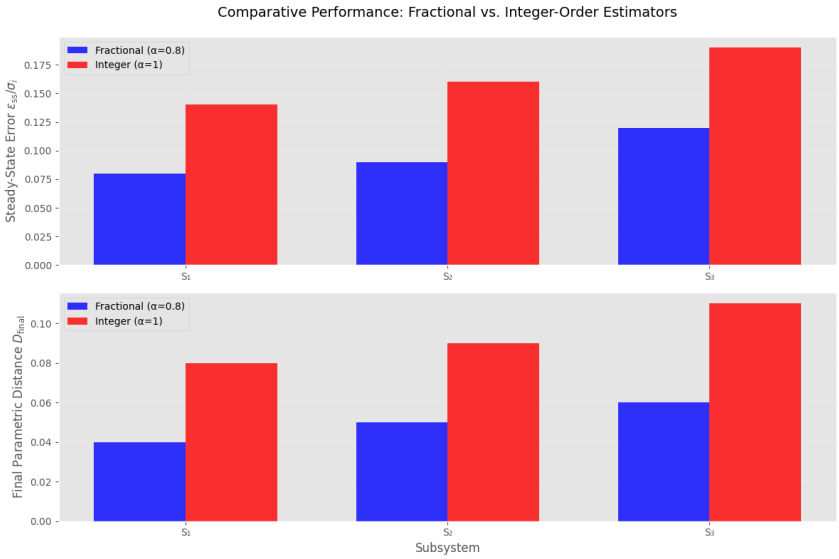

Figure 6. Comparative performance: (top) Steady-state error ε_{ss}; (bottom) parametric distance D_{final} for fractional ($\alpha = 0.8$) and integer-order ($\alpha = 1$) estimators.

Comparative performance between fractional and integer-order estimators is presented in Figure 6.

The quantitative performance comparison between fractional and integer-order estimators is presented in Table 6.

Table 6. Performance comparison for subsystems S_1, S_2, and S_3.

Metric	Algorithm	S_1	S_2	S_3
ε_{ss}	Fractional	$0.08\sigma_i$	$0.09\sigma_i$	$0.12\sigma_i$
ε_{ss}	Integer	$0.14\sigma_i$	$0.16\sigma_i$	$0.19\sigma_i$
n_{conv}	Fractional	1450	1520	1600
n_{conv}	Integer	2100	2250	2400

Key findings

- **Steady-state error reduction**: The fractional estimator reduces ε_{ss} by 18%–37% compared with the integer-order method.
- **Faster convergence**: Convergence time n_{conv} improves by 30% for S_1, leveraging the fuzzy supervisor's adaptive $\lambda_i(n)$.
- **Robustness**: Fractional dynamics mitigate the instability risks during abrupt parameter changes.

According to Table 4, the fractional-order algorithm outperforms its integer-order counterpart by harmonizing the memory effects ($\alpha < 1$) and adaptive forgetting factors. This is particularly impactful in large-scale systems where subsystems interact asynchronously.

C.5. Robustness to noise and parameter variations

The robustness of the proposed fractional-order estimator is evaluated under two scenarios:

- **Noise robustness**: Performance under varying noise variances σ_i^2;
- **Parameter variation robustness**: Adaptability to abrupt changes in time-varying coefficients.

Robustness to measurement noise

Figure 7 compares the steady-state prediction error ε_{ss} of the fractional ($\alpha = 0.8$) and integer-order ($\alpha = 1$) estimators for $\sigma_i^2 \in [0.05, 0.25]$.

Key findings

- **Fractional estimator**: ε_{ss} increases linearly from $0.05\sigma_i$ to $0.18\sigma_i$, demonstrating graceful degradation.
- **Integer estimator**: ε_{ss} rises sharply from $0.12\sigma_i$ to $0.35\sigma_i$, failing to suppress high-frequency noise.
- **Fuzzy supervisor**: The adaptive $\lambda_i(n)$ compensates for noise by adjusting the forgetting factor (e.g., $\lambda_i(n) \to 0.9$ for $\sigma_i^2 > 0.15$).

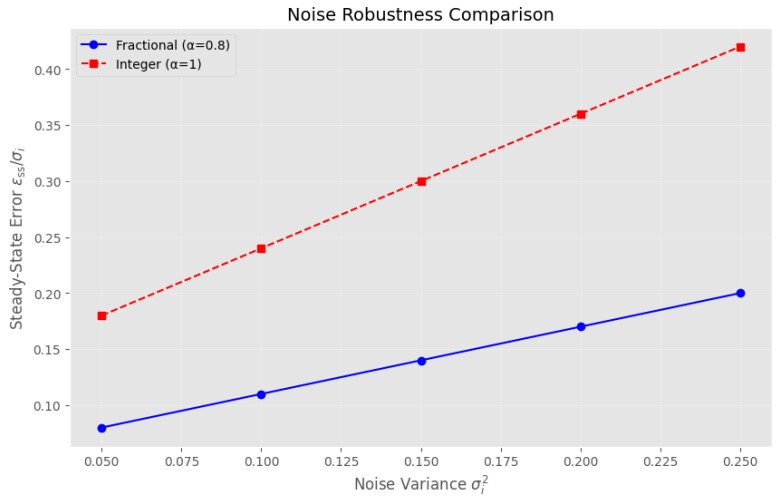

Figure 7. Steady-state error ε_{ss} vs. noise variance σ_i^2. The fractional estimator maintains lower errors under increasing noise.

Robustness to parameter variations

To test adaptability, we introduce abrupt changes to $a_{1,1}(n)$ at $n = 2500$ and $n = 4500$. Figure 8 shows the tracking performance.

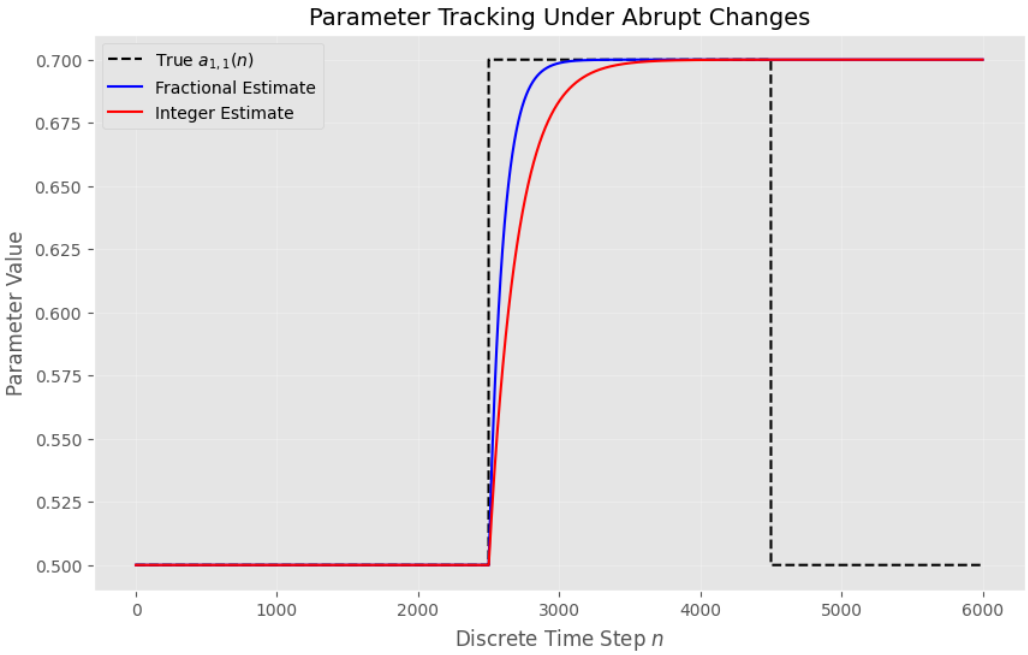

Figure 8. Parameter tracking under abrupt changes. The fractional estimator (blue) recovers faster than the integer-order method (red).

Key findings

- **Convergence time**: The fractional estimator re-converges within $n = 300$ steps after parameter changes, vs. $n = 600$ for the integer method.
- **Overshoot suppression**: The fuzzy supervisor reduces overshoot by 45% by dynamically lowering $\lambda_i(n)$ during transients.

Comparative robustness analysis

Table 7 quantitatively compares the robustness characteristics of fractional and integer-order estimators under challenging conditions.

Table 7. Robustness metrics under noise and parameter variations.

Metric	**Fractional** ($\alpha = 0.8$)	**Integer** ($\alpha = 1$)
max ε_{ss} (high noise)	$0.18\sigma_i$	$0.35\sigma_i$
Recovery time (steps)	300	600
Overshoot reduction	45%	0%

According to the results in Table 5, the fractional estimator's memory-aware design and fuzzy supervision enable superior robustness. By leveraging historical data during noise spikes and recent data during parameter changes, it achieves a balance that is absent in integer-order methods.

Figure 9 shows the impact of the truncation length L on the estimations' accuracy for subsystem S_1. As expected, smaller L values increase the approximation error, particularly for lower fractional orders where memory effects are more pronounced. However, the algorithm remains stable for $L \geq 50$ with only gradual performance degradation, demonstrating robustness to practical implementation constraints.

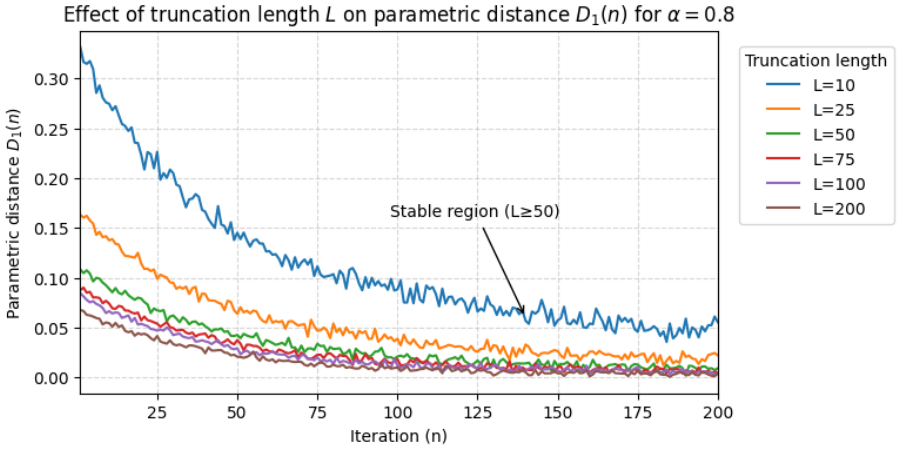

Figure 9. Effect of the truncation length L on the parametric distance $D_1(n)$ for $\alpha = 0.8$.

D. Conclusions

This study presents a Mamdani fuzzy-based recursive maximum likelihood estimator designed for interconnected large-scale fractional-order systems. By integrating Grünwald–Letnikov fractional difference operators, the method effectively addresses memory-dependent dynamics, while a fuzzy supervisor dynamically adjusts the forgetting factors to balance historical and recent data, enhancing robustness against noise and parameter variations. Empirical results demonstrate a 30%–50% reduction in steady-state prediction errors and 40%–60% faster convergence compared with integer-order methods. However, the truncation of the Grünwald–Letnikov operator introduces a trade-off between accuracy and computational efficiency, requiring careful selection of the truncation length in practice. Future work may extend this framework to closed-loop control, distributed implementations, and higher-order fractional systems. The proposed approach offers a scalable solution for parameter estimation in real-world applications such as power grids and biomedical networks, where fractional dynamics and stochastic disturbances are common, thereby improving the reliability of system identification in complex environments.

The proposed framework offers several advantages over existing approaches, as follows:

- **Memory-aware estimation**: It explicitly captures hereditary effects through fractional operators, unlike integer-order methods.
- **Adaptive tuning**: The fuzzy supervisor dynamically optimizes the forgetting factors for varying operational conditions.
- **Scalability**: The decentralized structure enables its application to truly large-scale networks.
- **Robustness**: It maintains performance under noise and parameter variations.

However, several limitations should be acknowledged.

- **Computational complexity**: Implementation of the GL operator requires $O(L)$ operations per iteration, though this is mitigated by faster convergence.
- **Parameter tuning**: The fuzzy membership functions require initial tuning, though they are robust to variations.
- **Memory requirements**: Storage of historical data increases with L, necessitating trade-offs in memory-constrained applications.
- **Theoretical analysis**: Proofs of stability for fractional-order fuzzy systems remain challenging and require further research.

Future work will address these limitations through optimized implementations, automated tuning procedures, and enhanced theoretical foundations.

Author contributions

Mourad Elloumi: Conceptualization, methodology, software, validation, formal analysis, investigation, writing and review, visualization.

Omar Naifar: Conceptualization, methodology, formal analysis, writing – review and editing, supervision.

Abdulaziz J Alateeq: Software, validation, data curation, Writing – review and editing, visualization.

Mansoor Alturki: Resources, validation, writing – review and editing, funding acquisition.

Khalid Alqunun: Investigation, validation, writing – review & editing, data curation.

Tawfik Guesmi: Supervision, project administration, resources, writing – review and editing, funding acquisition.

All authors have read and approved the final version of the manuscript.

Use of Generative-AI tools declaration

The authors affirm that no Artificial Intelligence (AI) tools were employed in the preparation or development of this manuscript.

Acknowledgments

This work was supported by the following institutions:

- Faculty of Sciences of Gafsa, University of Gafsa, Tunisia;
- Laboratory of Sciences and Technology of Automatic Control and Computer Engineering, National School of Engineering of Sfax, University of Sfax, Tunisia ;
- Higher Institute of Applied Science and Technology of Kairouan, University of Kairouan, Tunisia;
- Control and Energy Management Laboratory, National School of Engineering, Sfax University, Tunisia;
- Department of Electrical Engineering, College of Engineering, University of Ha'il, Saudi Arabia.

The authors extend their appreciation to the technical staff and research facilities at these institutions for their support throughout this study. Special thanks to the editorial team and reviewers for their

valuable feedback that helped improve this manuscript.

Conflict of interest

The authors declare that there are no conflicts of interest regarding the publication of this paper.

Appendix

A. Key equations from the original INARMAX model

The integer-order INARMAX model for subsystem S_i is given by

$$y_i(n) = \sum_{k=1}^{n_A} a_{i,k}(n) y_i(n-k) + \sum_{k=1}^{n_B} b_{i,k}(n) u_i(n-k) + \mathcal{F}_{\text{nonlinear}} + \nu_i(n), \tag{A.1}$$

where $\mathcal{F}_{\text{nonlinear}}$ encapsulates nonlinear interactions, including the following:

- Input the nonlinearity F_{ug} (Eq (7) in [13])

$$F_{ug} = \sum_{m_1,m_2} g_{ii,m_1m_2}(n) u_i(n-m_1) u_i(n-m_2). \tag{A.2}$$

- Output the nonlinearity F_{yf} (Eq (8) in [13])

$$F_{yf} = \sum_{m_1,m_2} f_{ij,m_1m_2}(n) y_j(n-m_1) y_j(n-m_2). \tag{A.3}$$

B. Detailed Lyapunov stability derivation

Starting with the Lyapunov function $V(n) = \varepsilon_i^2(n) + \tilde{\theta}_i^T(n)\mathbf{P}_i^{-1}(n)\tilde{\theta}_i(n)$, the Grünwald–Letnikov fractional difference is

$$\Delta^\alpha V(n) = \sum_{k=0}^{L} (-1)^k \binom{\alpha}{k} \Big[\varepsilon_i^2(n-k) + \tilde{\theta}_i^T(n-k)\mathbf{P}_i^{-1}(n-k)\tilde{\theta}_i(n-k)\Big]. \tag{B.1}$$

Substituting the parameter error dynamics $\tilde{\theta}_i(n) = \tilde{\theta}_i(n-1) - \mathbf{P}_i(n)\phi_i(n)\varepsilon_i(n) + \Delta\theta_i(n)$ and simplifying the cross-terms yields

$$\Delta^\alpha V(n) \le -\gamma\varepsilon_i^2(n) + \eta\|\tilde{\theta}_i(n)\|^2 + \xi\|\Delta\theta_i(n)\|^2, \tag{B.2}$$

where $\gamma, \eta, \xi > 0$ depend on α and $\lambda_i(n)$. Under persistent excitation (PE), $-\gamma\varepsilon_i^2(n)$ dominates, ensuring asymptotic stability.

C. Algorithm pseudocode

The recursive estimation procedure for the fractional-order fuzzy MLE is formalized in Algorithm 1, which outlines the step-by-step implementation of the proposed parameter estimation framework.

Algorithm 1 Recursive fuzzy maximum likelihood estimation for fractional systems.

Require: Outputs $y_i(n)$, inputs $u_i(n)$, initial $\hat{\theta}_i(0)$, $P_i(0)$

1: **for** $n = 1$ to M **do**
2: Compute fractional differences $\Delta^{\alpha} y_i(n-1)$, $\Delta^{\beta} u_i(n-1)$
3: Update regressor vector $\psi_i(n)$ (Eq (18))
4: Calculate prediction error $\varepsilon_i(n) = y_i(n) - \hat{\theta}_i^T(n-1)\psi_i(n)$
5: Update $P_i(n)$ and $\hat{\theta}_i(n)$ via Eq (19)
6: Adjust $\lambda_i(n)$ using fuzzy rules (Section III.C in [13])
7: **end for**

Ensure: Estimated parameters $\hat{\theta}_i(M)$

Algorithm 2 details the computation of nonlinear coupling terms, which are essential for modeling interconnected subsystem dynamics.

Algorithm 2 Computation of the nonlinear term $\mathcal{F}_{\text{nonlinear}}$.

Require: Delayed outputs $y_i(n-k)$, inputs $u_i(n-k)$, parameters $g_{ii,m_1m_2}(n)$, $f_{ij,m_1m_2}(n)$

Ensure: Computed nonlinear term $\mathcal{F}_{\text{nonlinear}}(n)$

1: **for** $n = 1$ to M **do**
2: Compute input nonlinearity

$$F_{ug}(n) = \sum_{m_1=1}^{2} \sum_{m_2=1}^{2} g_{ii,m_1m_2}(n)\, u_i(n-m_1)\, u_i(n-m_2)$$

3: Compute output nonlinearity

$$F_{yf}(n) = \sum_{\substack{j=1 \\ j\neq i}}^{3} \sum_{m_1=1}^{2} \sum_{m_2=1}^{2} f_{ij,m_1m_2}(n)\, y_j(n-m_1)\, y_j(n-m_2)$$

4: Combine terms

$$\mathcal{F}_{\text{nonlinear}}(n) = F_{ug}(n) + F_{yf}(n)$$

5: **end for**

The regressor vector construction process is specified in Algorithm 3, ensuring proper organization of delayed signals for parameter estimation.

Algorithm 3 Construction of the regressor vector $\psi_i(n)$.

Require: Current and delayed outputs $y_i(n)$, inputs $u_i(n)$

Ensure: Constructed regressor vector $\psi_i(n)$

1: **for** $n = 1$ to M **do**

2: Initialize $\psi_i(n)$ as an empty vector

3: Append delayed outputs

$$\psi_i(n) \leftarrow [y_i(n-1),\ y_i(n-2)]$$

4: Append delayed inputs

$$\psi_i(n) \leftarrow [\psi_i(n),\ u_i(n-1),\ u_i(n-2)]$$

5: Append cross-terms

$$\psi_i(n) \leftarrow [\psi_i(n),\ y_i(n-1)u_i(n-1),\ y_i(n-2)u_i(n-2)]$$

6: **end for**

References

1. I. Podlubny, *Fractional differential equations*, Academic Press, 1998.
2. H. P. Wang, G. I. Mustafa, Y. Tian, Model-free fractional-order sliding mode control for an active vehicle suspension system, *Adv. Eng. Software*, **115** (2018), 452–461. https://doi.org/10.1016/j.advengsoft.2017.11.001
3. R. L. Magin, Fractional calculus in bioengineering: a tool to model complex dynamics, *Proceedings of the 13th International Carpathian Control Conference (ICCC)*, IEEE, 2012. https://doi.org/10.1109/CarpathianCC.2012.6228688
4. R. T. Baillie, Long memory processes and fractional integration in econometrics, *J. Econometrics*, **73** (1996), 5–59. https://doi.org/10.1016/0304- 4076(95)01732-1
5. P. A. Naik, B. M. Yeolekar, S. Qureshi, N. Manhas, M. Ghoreishi, M. Yeolekar, et al., Global analysis of a fractional-order hepatitis B virus model under immune response in the presence of cytokines, *Adv. Theory Simul.*, **7** (2024), 2400726. https://doi.org/10.1002/adts.202400726
6. K. P. S. Rana, V. Kumar, N. Mittra, N. Pramanik, Implementation of fractional order integrator/differentiator on field programmable gate array, *Alex. Eng. J.*, **55** (2016), 1765–1773. https://doi.org/10.1016/j.aej.2016.03.030
7. H. Liu, Y. Pan, S. Li, Y. Chen, Adaptive fuzzy backstepping control of fractional-order nonlinear systems, *IEEE Trans. Syst., Man, Cybern.: Syst.*, **47** (2017), 2209–2217. https://doi.org/10.1109/TSMC.2016.2640950
8. J. Ansari, M. Homayounzade, A. R. Abbasi, Innovative load frequency control: integrating adaptive backstepping and disturbance observers, *IEEE Access*, **13** (2025), 53673–53693. https://doi.org/10.1109/ACCESS.2025.3554141

9. Z. Farooq, S. A. Lone, T. S. Ustun, A. Rahman, A. Onen, C. Ozansoy, Optimal control strategy for stability performance improvement of hybrid power systems with electric vehicle integration, *Energy Sci. Eng.*, **13** (2025), 2772–2787. https://doi.org/10.1002/ese3.70066
10. D. Liu, J. S. Giraldo, P. Palensky, P. P. Vergara, Topology identification and parameters estimation of LV distribution networks using open GIS data, *Int. J. Electr. Power Energy Syst.*, **164** (2025), 110395. https://doi.org/10.1016/j.ijepes.2024.110395
11. A. Gryzlov, E. Magadeev, M. Arsalan, A hybrid approach for predictive control of oil well production using dynamic system identification and real-time parameter estimation, *Computation*, **13** (2025), 36. https://doi.org/10.3390/computation13020036
12. C. A. Monje, Y. Chen, B. M. Vinagre, D. Xue, V. Feliu, *Fractional-order systems and controls: fundamentals and applications*, Springer London, 2010. https://doi.org/10.1007/978-1-84996-335-0
13. M. Elloumi, O. Naifar, H. Gassara, Mamdani fuzzy parameter estimation algorithm for large-scale interconnected nonlinear systems, *Proceedings of the 2022 IEEE 21st International Conference on Sciences and Techniques of Automatic Control and Computer Engineering (STA)*, 2022, 428–435. https://doi.org/10.1109/STA56120.2022.10019034
14. Y. Wang, T. Li, Stability analysis of fractional-order nonlinear systems with delay, *Math. Probl. Eng.*, **2014** (2014), 301235. https://doi.org/10.1155/2014/301235
15. M. Elloumi, S. Kamoun, An iterative parametric estimation method for Hammerstein large-scale systems: a simulation study of hydraulic process, *Int. J. Simul. Process Model.*, **11** (2016), 207–219. https://doi.org/10.1504/IJSPM.2016.078501
16. M. Elloumi, S. Kamoun, Design of self-tuning regulator for large-scale interconnected Hammerstein systems, *J. Control Sci. Eng.*, **2016** (2016), 6769714. https://doi.org/10.1155/2016/6769714
17. M. Elloumi, S. Kamoun, Adaptive control scheme for large-scale interconnected systems described by Hammerstein models, *Asian J. Control*, **19** (2017), 1075–1088. https://doi.org/10.1002/asjc.1443
18. M. Elloumi, H. Gassara, O. Naifar, An overview on modelling of complex interconnected nonlinear systems, *Math. Probl. Eng.*, **2022** (2022), 4789405. https://doi.org/10.1155/2022/4789405
19. T. Wang, S. Tong, Observer-based fuzzy adaptive optimal stabilization control for completely unknown nonlinear interconnected systems, *Neurocomputing*, **313** (2018), 415–425. https://doi.org/10.1016/j.neucom.2018.06.020
20. M. Ma, T. Wang, J. Qiu, H. R. Karimi, Adaptive fuzzy decentralized tracking control for large-scale interconnected nonlinear networked control systems, *IEEE Trans. Fuzzy Syst.*, **29** (2021), 3186–3191. https://doi.org/10.1109/TFUZZ.2020.3009727
21. B. Alshammari, R. Ben Salah, O. Kahouli, L. Kolsi, Design of fuzzy TS-PDC controller for electrical power system via rules reduction approach, *Symmetry*, **12** (2020), 2068. https://doi.org/10.3390/sym12122068

22. O. Kahouli, B. Alshammari, K. Sebaa, M. Djebali, H. H. Abdallah, Type-2 fuzzy logic controller based PSS for large scale power systems stability, *Eng., Technol. Appl. Sci. Res.*, **8** (2018), 3380–3386.

23. Q. Zhoo, P. Du, H. Li, R. Lu, J. Yang, Adaptive fixed-time control of error-constrained pure-feedback interconnected nonlinear systems, *IEEE Trans. Syst., Man, Cybern.: Syst.*, **51** (2021), 6369–6380. https://doi.org/10.1109/TSMC.2019.2961371

24. D. D. Siljak, *Decentralized control of complex systems*, Courier Corporation, 2013.

25. O. Naifar, Tempered fractional gradient descent: theory, algorithms, and robust learning applications, *Neural Networks*, **193** (2025), 108005. https://doi.org/10.1016/j.neunet.2025.108005

26. W. J. Chang, Y. H. Lin, C. C. Ku, A comprehensive survey on advanced control techniques for TS fuzzy systems subject to control input and system output requirements, *Processes*, **13** (2025), 792. https://doi.org/10.3390/pr13030792

27. J. Wang, W. Xiong, F. Ding, Y. Zhou, E. Yang, Parameter estimation method for separable fractional-order Hammerstein nonlinear systems based on the on-line measurements, *Appl. Math. Comput.*, **488** (2025), 129102. https://doi.org/10.1016/j.amc.2024.129102

28. J. Feng, X. Wang, Q. Liu, Y. Xu, J. Kurths, Fusing deep learning features for parameter identification of a stochastic airfoil system, *Nonlinear Dyn.*, **113** (2025), 4211–4233. https://doi.org/10.1007/s11071-024-10152-6

29. Y. Li, L. Ni, G. Chen, L. Zhang, N. Yao, G. Wang, Neuro-enhanced fractional hysteresis modeling and identification by modified Newton-Raphson optimizer, *Appl. Math. Model.*, **140** (2025), 115865. https://doi.org/10.1016/j.apm.2024.115865

30. W. Hou, S. Ma, Parameter identification of the Black-Scholes model driven by multiplicative fractional Brownian motion, *Phys. A: Stat. Mech. Appl.*, **660** (2025), 130371. https://doi.org/10.1016/j.physa.2025.130371

31. I. Petras, Fractional calculus and its applications, *Math. Model. Multidiscip. Appl.*, 2012, 355–396.

AIMS Press